

## STRUCTURAL CHARACTERIZATION OF COBALTDOPED BISMUTH FERRITE MATERIALS

Aye Aye Khaine<sup>1</sup>, Lei Lei Aung<sup>2</sup>, Myo Myint Aung<sup>3</sup> and Min Maung Maung<sup>4</sup>

### Abstract

Bismuth ferrite (BiFeO<sub>3</sub>) and cobalt doped BiFeO<sub>3</sub>(BiFe<sub>1-x</sub>Co<sub>x</sub>O<sub>3</sub>) materials were prepared by combustion method. The X-ray diffraction (XRD) method confirmed crystalline phase and crystalline size of these materials. The average crystallite size was obtained 30.26 nm. The shifting of peaks to higher angles was observed in cobalt doped BiFeO<sub>3</sub>. The formation of bonding structure was also identified by Fourier Transform infrared Spectroscopy (FTIR), it confirms the existence of Fe-O and Bi-O bands. The energy band gap was also evaluated from the measurement of UV spectrophotometer. It was observed that the increase in optical band gap with increasing in cobalt doping concentration in the BiFeO<sub>3</sub> structure.

**Keywords:** bismuth ferrite; Auto-combustion technique; XRD; crystallite size; FTIR; FWHM.

### Introduction

Multiferroic oxides have the unique properties of both ferromagnetism and ferroelectricity in a single crystal. This opens broader applications in transducers, magnetic field sensors and information storage industry. These include BiFeO<sub>3</sub>, BiMnO<sub>3</sub>, TbMnO<sub>3</sub>, TbMn<sub>2</sub>O<sub>5</sub>, YMnO<sub>3</sub>, LuFeO<sub>4</sub> and Ni<sub>3</sub>B<sub>7</sub>O<sub>13</sub>. Among these oxides BiFeO<sub>3</sub> (BFO) is the only material which gives ferroelectricity and antiferromagnetism at room temperature. Due to coexistence of both ferromagnetism and ferroelectricity in the same material, it is expected to exhibit ferromagnetic & ferroelectric properties or a coupling of these two properties in a single material. This increases the current range of application and moreover interesting physics may be observed.

A single phase multiferroic material is one that possesses two of the three ferroic " properties i.e ferroelectricity, ferromagnetism and ferroelasticity. Generally current trend is to exclude the requirement for ferroelastic property. Magnetoelectric coupling describes the coupling between magnetic and electric order parameters. BiFeO<sub>3</sub> is the only prototype among all other multiferroic oxides which shows both ferromagnetism and ferroelectricity in a single crystal above room temperature. It has ferroelectric Curie temperature  $T_c = 1143\text{K}$  and antiferromagnetic Neel temperature  $T_N = 643\text{K}$ . The ions responsible for the production of ferroelectricity and magnetism are Bi<sup>3+</sup> and Fe<sup>3+</sup> ions. Ferroelectricity is produced due to Bi<sup>3+</sup> and antiferromagnetism is due to Fe<sup>3+</sup> ions. It is having rhombohedrally distorted perovskite structure with R3c space group at room temperature. Bi<sup>3+</sup> ion occupy the corner position, Fe<sup>3+</sup> in the body centred position, and O<sub>2</sub><sup>-</sup> in allface centred position. The lattice parameters are  $a = 5.587 \text{ \AA}$ ,  $b = 5.587 \text{ \AA}$  and  $c = 13.867 \text{ \AA}$  with  $\alpha = \beta = 90^\circ$  and  $\gamma = 120^\circ$ . The Orthorhombic unit cell contains 6 formulas.

In the present work, cobalt doped bismuth ferrite was prepared by sol-gel combustion method. The XRD, SEM and FTIR analyses indicate the formation of single phase materials with particle size in the nanometer range. The energy band gap measurement was also done by using UV spectrophotometer.

---

<sup>1</sup> Dr, Associate Professor, Department of Physics, Yangon University of Distance Education.

<sup>2</sup> Dr, Associate Professor, Department of Physics, Yangon University of Distance Education.

<sup>3</sup> Dr, Associate Professor, Department of Physics, Yangon University of Distance Education.

<sup>4</sup> Dr, Associate Professor, Department of Physics, University of Yangon.

## Experimental Procedure

The samples were prepared by sol – gel combustion route. The fuel chosen for the synthesis was ethylene glycol. The stoichiometric amount of  $\text{Bi}(\text{NO}_3)_3 \cdot 5 \text{H}_2\text{O}$  salt was dissolved in the mixture of ethylene glycol and deionized water by constant stirring at the temperature 40-50°C. Then  $\text{Fe}(\text{NO}_3)_3 \cdot 9\text{H}_2\text{O}$  salt was added to the mixture. Now the colour of the solution changes from colour less to brick red then red and finally blackish red. After 1 hour of continuous stirring the solution is heated with stirring at a temperature of 70°C. After 3 hours of heating and stirring the solution became transparent gel. Then after few minutes and in some elevated temperature yellow colour precipitation occurred. This precipitate was found to be hygroscopic when left for 10 hours. So the sample was then again heated at a temperature 100°C, to vaporize all the water content from the sample. After some time the powder in the bottom of beaker turned black, gradually the whole powder become blackish. The black powder was also found to be hygroscopic. The powder collected was then calcined for 4 hours at a temperature of 900°C. The furnace heating rate is maintained as 4° / minute. After cooling, the sample is collected from the furnace and is grinded by agate-mortar. The grinded powder is now ready for necessary characterization. To obtain the Co doped BFO,  $\text{Co}(\text{NO}_3)_2 \cdot 6\text{H}_2\text{O}$  is added after  $\text{Bi}(\text{NO}_3)_3 \cdot 5 \text{H}_2\text{O}$  then followed by  $\text{Fe}(\text{NO}_3)_3 \cdot 9\text{H}_2\text{O}$ .

## Result and Discussions

### XRD Analysis:

Phase analysis was studied using the room temperature powder X-ray diffraction with filtered 0.154 nm Cu K $\alpha$  radiation. Samples were scanned in a continuous mode from 20°–80° with a scanning rate of 30/minute. XRD patterns of Co doped  $\text{BiFeO}_3$  (BCFO) ceramic calcined at 900°C were shown in the figure 1. The prominent peaks in XRD plot were indexed to various hkl planes of BCFO, indicating formation of BCFO. Besides these prominent peaks, some other peaks of low intensity are also observed, which do not belong to BFO. The literature survey of BFO synthesis relates these impurity peaks to be that of  $\text{Bi}_2\text{Fe}_4\text{O}_9$  and  $\text{Bi}_{25}\text{FeO}_{39}$ . The appearance of these extra phases at 900°C could be due to large bismuth loss at higher temperature. These results indicate that on cobalt doping up to 5 mol % at Fe site, the Orthorhombic structure of BFO does not change appreciably, except increase in  $\text{Bi}_{25}\text{FeO}_{39}$  and  $\text{Bi}_2\text{Fe}_4\text{O}_9$  impurity phases at 330 and 280. The intensity of impurity peaks increases with increase in doping concentration, indicating increasing concentration of impurity phases. The crystallite parameter and the average crystallite size were listed in the table 1.

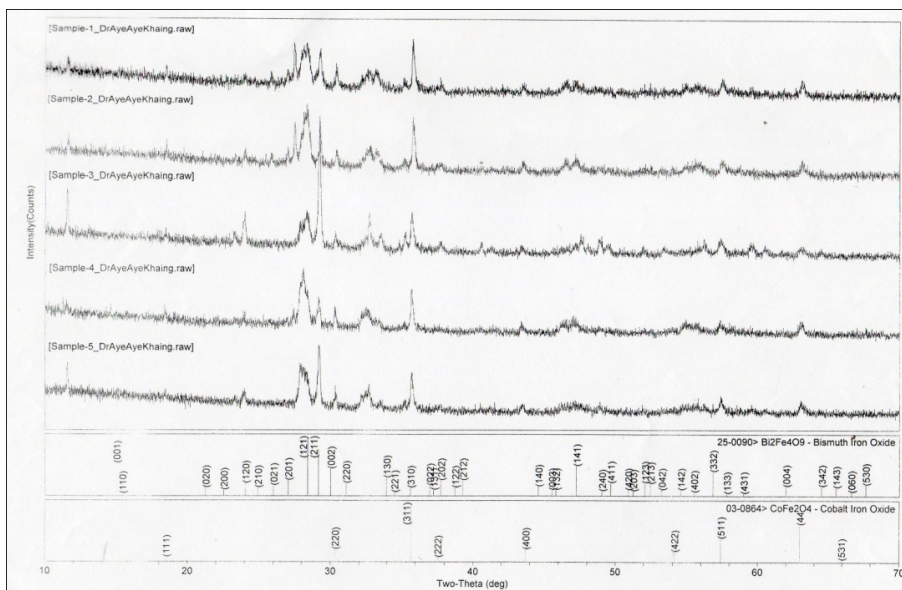


**Figure 1** The XRD pattern of Co doped BiFeO<sub>3</sub> materials Lattice parameters, FWHM and crystallite size of BiFe<sub>1-x</sub>Co<sub>x</sub>O<sub>3</sub>

Prepared samples	a (Å)	b (Å)	c (Å)	FWHM	Crystallite size (nm)
CoFe <sub>0.9</sub> Ni <sub>0.1</sub> O <sub>3</sub>	6.4500	9.6271	5.8773	0.299	27.6485
CoFe <sub>0.8</sub> Ni <sub>0.2</sub> O <sub>3</sub>	7.8436	8.8917	5.9115	0.303	27.282
CoFe <sub>0.7</sub> Ni <sub>0.3</sub> O <sub>3</sub>	6.6096	9.6105	5.3578	0.274	30.133
CoFe <sub>0.6</sub> Ni <sub>0.4</sub> O <sub>3</sub>	7.5978	8.8636	5.9532	0.242	29.240
CoFe <sub>0.5</sub> Ni <sub>0.5</sub> O <sub>3</sub>	7.7436	9.0019	5.8609	0.223	37.031

**TGA-DTA analysis:**

The TGA-DTA analysis of all the three samples was carried out using thermo gravimetric analysis and differential scanning calorimetric (DSC-TG) by heating the sample at 10 °C/min. The plot was shown in the figure 2. Figure showed the TGA-DTA analysis of unleached & calcined BFO, by taking heat flow and mass loss in Y – axis and temperature in X – axis. The TGA plot of BFO reveals a broader decrease in mass near 100°C due to evaporation of water molecules. As gradually increase the temperature there was a considerable loss of mass around 300 - 400°C, which is a broader one. It may be due to bismuth loss around this temperature, as bismuth is having boiling point of 275°C. The mass was gradually decreasing and around 350°C there was an increase in mass which may be due to formation of some new compounds by reaction of the sample with the atmosphere. The broader depression around 430°C may be due to melting of the compound and presence of some liquid phase. The broader endothermic peak around 280°C showed there was a consider able amount of liquids are formed at this temperature. The mass loss plot showed there is a continuous decrease of mass as increase the temperature and around 500°C the mass loss rate was decreased and again it was saturated.

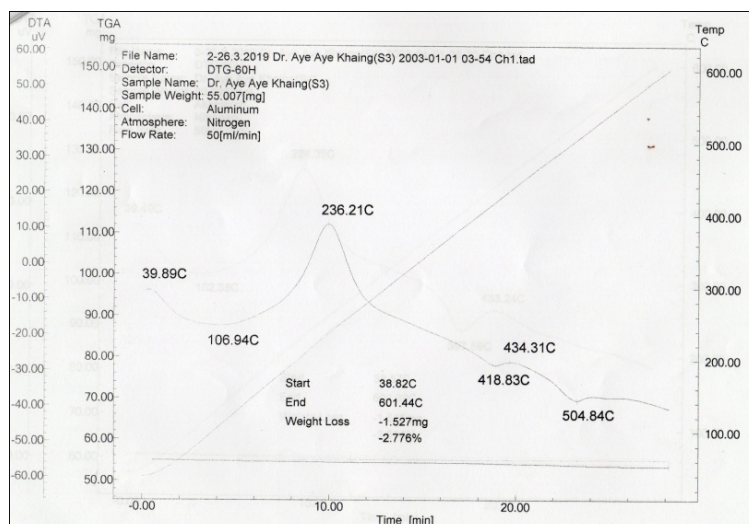


**Figure 2** The TGA-DTA plot of Co doped  $\text{BiFeO}_3$  materials

### SEM Analysis:

Microstructural features were studied using Scanning Electron Microscope. The SEM microstructure of all samples is given in figure 3. All the samples are leached and sintered. The samples were in agglomerated form and it had no definite shape and size. The microstructure of the samples sintered showed appearance of sharp features and blocks of various shapes and sizes (100 nm to  $1\mu\text{m}$ ). Another important thing to observe while comparing the micrographs of the sintered samples that the grain size goes on increasing as increase the doping concentration of Cobalt. This result is well agreement with the x-ray diffraction data, which showed decrease in lattice volume with cobalt concentration.

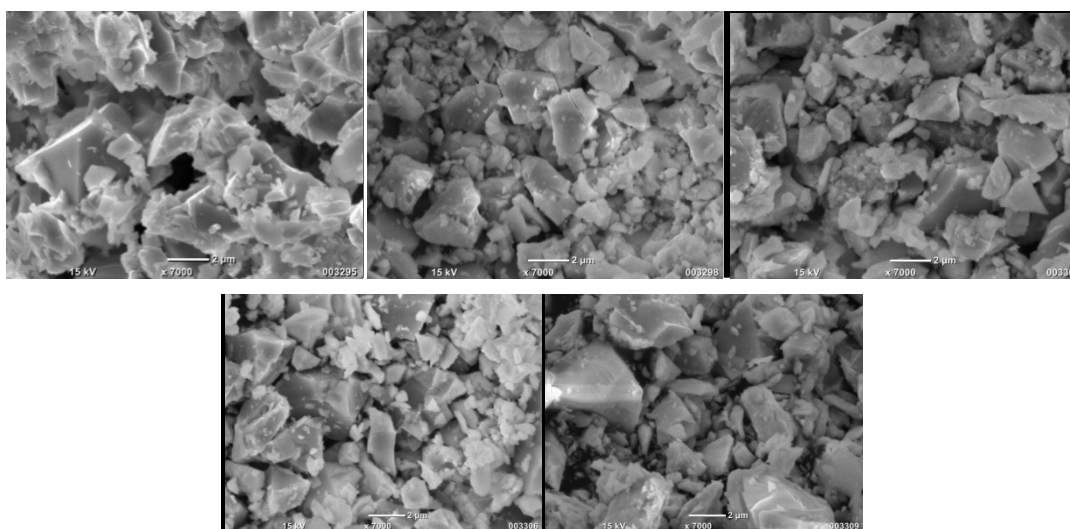


**Figure 3** The SEM images of Co doped  $\text{BiFeO}_3$  materials

### FTIR Analysis

The FT-IR spectra of  $\text{CoBi}_x\text{Fe}_{2-x}\text{O}_4$ , (where  $x = 0.1, 0.2, 0.3, 0.4, 0.5$ ) nano ferrite particles, synthesised at room temperature was represented in the figure 4. As shown, four characteristic IR peaks together with some weak peaks appeared for BCFO precursor using citric acid as chelating. The above broad frequency range corresponds to O-H stretching, H-O-H bending

vibration of water molecules and spinal structure with sub-lattices respectively Samples had two sharp and one wide IR peaks, which correspond to the stretching vibrations of C=O and –OH. The IR wide peaks located at  $2370\text{ cm}^{-1}$  were assigned to the stretching vibrations of structural hydroxyl (OH) groups, and the intense peaks at  $1368.52\text{ cm}^{-1}$  were assigned to the stretching vibrations of C=O. The IR peaks located at  $1368.52\text{ cm}^{-1}$  were attributed to the symmetry bending vibration of C–H. The IR peaks below  $1000\text{ cm}^{-1}$  (such as 617, 591, 683,898, and  $990\text{ cm}^{-1}$ ) were corresponding to the vibrations bonds of Bi–O or Fe–O, respectively. The presence of frequency bands in this specific range explained the normal mode of vibration of tetrahedral cluster was higher than that of octahedral cluster in the spinel ferrites. The highest one corresponds to the intrinsic stretching vibrations of the metal at the tetrahedral site, whereas the lowest band was assigned to octahedral-metal stretching. This difference between the tetrahedral and octahedral clusters of spinel ferrite was because of the variation in distance between  $\text{Fe}^{3+}\text{-O}^{2-}$  ions in tetrahedral and octahedral sites. The wave band  $\nu_1$  showed an increase in the values with increase in Bi concentration which may be due to dissimilarity in the cations-oxygen bond length.

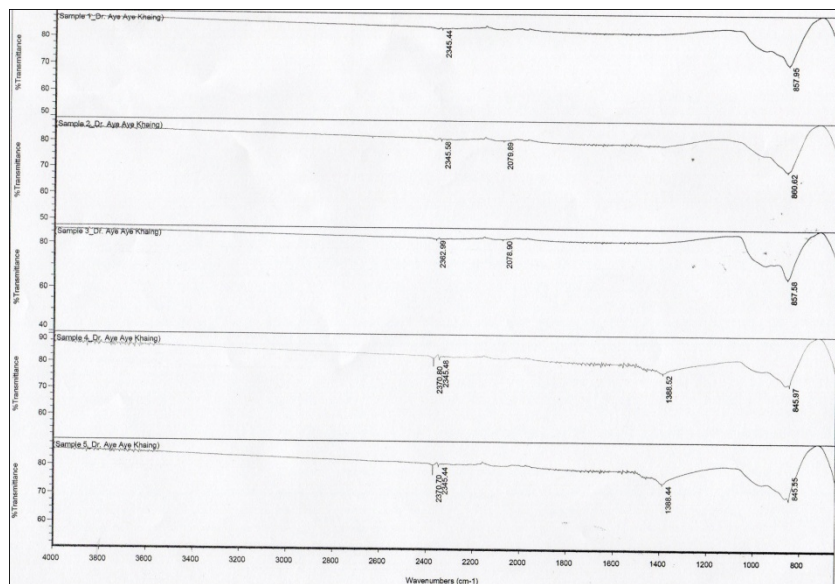


**Figure 4** The FTIR spectrums of Co doped  $\text{BiFeO}_3$  materials

### Energy Gap measurement

The energy band gap of the material was measured using Tauc relation  $(\alpha h\nu) = A(h\nu - E_g)^n$  where  $\alpha$  was the absorption coefficient,  $A$  was an energy independent constant of the absorption frequency,  $h$  was Planck's constant,  $E_g$  was band gap,  $m$  was frequency of incident photon and  $n$  is the index which depends on electronic transitions responsible for optical absorption. The value of optical energy band gap  $E_g$  has been calculated for the all samples by  $(\alpha h\nu)^2$  vs  $h\nu$  plots. The values of  $E_g$  for different samples were found by extrapolating the linear portion to the  $h\nu$  determine the energy band gap  $E_g$  to be from 4.5 to 5.2 eV.



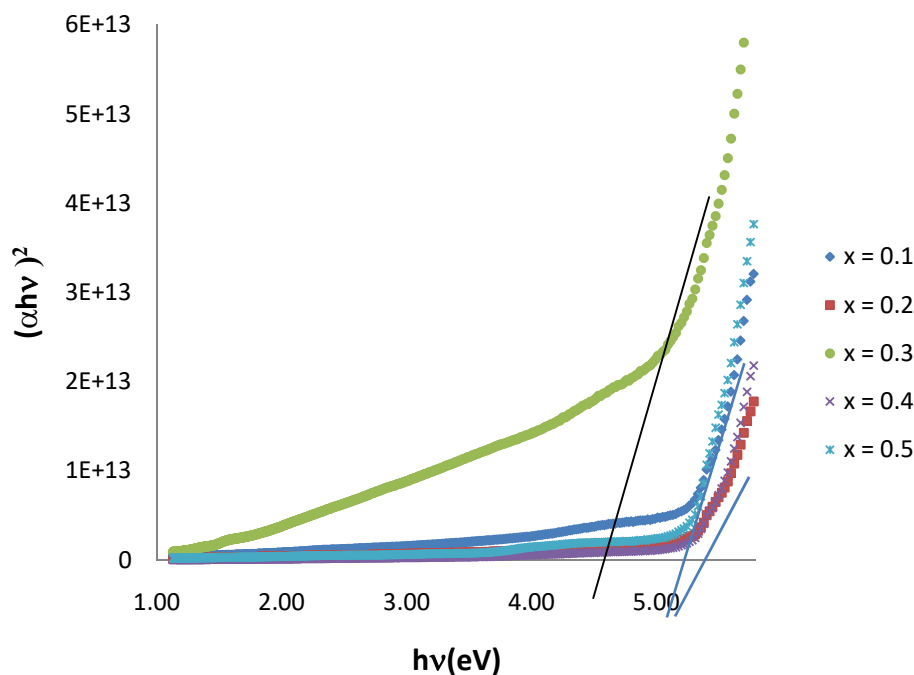


**Figure 5** The energy band gap of Co doped BiFeO<sub>3</sub> materials

### Conclusion

The samples were successfully prepared by sol-gel combustion synthesis method. Small amount of impurity phases are observed by x-ray diffraction results. The lattice parameters are  $a = 7.8436\text{\AA}$ ,  $b = 8.8917\text{\AA}$ ,  $c = 5.9115\text{\AA}$  and the crystal structure is Orthorhombic. The impurity phase grew with temperature from the literature survey, the impurity phases could be indexed to Bi<sub>2</sub>Fe<sub>4</sub>O<sub>9</sub> and Bi<sub>25</sub>FeO<sub>39</sub>. The cobalt doped BFO also found to be having impurity phases and it increases with increase in concentration of cobalt. Upon co-doping, the lattice volume of BFO decreases with cobalt concentration. This may be due to smaller ionic radius of cobalt (74 pm) than that of iron (78pm). From the SEM images of the BFO unsintered powder it is observed the powder is agglomerated and when this powder is sintered at 900°C and the SEM image revealed grains of tiny block with grain size varying from 100nm to 1μm. With increase in cobalt concentration there was shrinkage in grain size. The IR peaks below 1000 cm<sup>-1</sup> were corresponding to the vibrations bonds of Bi–O or Fe–O, respectively. This difference between the tetrahedral and octahedral clusters of spinel ferrite was because of the variation in distance between Fe<sup>3+</sup>-O<sup>2-</sup> ions in tetrahedral and octahedral sites. The wave band  $\nu_1$  showed an increase in the values with increase in Bi concentration which may be due to dissimilarity in the cations-oxygen bond length. The energy band gap  $E_g$  is the range of 4.7eV to 5.2eV for prepared samples.

## **Acknowledgement**

We are deeply grateful to Pro-Rector Dr Tin Mg Hla, Yangon University of Distance Education, for her kind permission to carry out our research work. We would like to thank Professor Dr Moh Moh, Head of Department of Physics and Professor Dr Mar-lar Myint, Department of Physics, Yangon University of Distance Education, for their kind permission to carry out this research work. We wish to express our sincere thanks to everyone who gave suggestion and help to make this research reality.

## **References**

Ahmad S et al, 2004, "Ferroelectric Ceramics Processing Properties and Applications", Department of Ceramic Science and Engineering, Rutgers University: USA

"Instruction Manual LCR meter GW 820", USA

Moulson A J & Herbert J M, 1997, "Electroceramic Materials Properties Applications", New Delhi: Thomson Press

Suryanarayana C. and Norton M. G. (1998), X-ray Diffraction A Practical Approach, (New York: Plenum)

Tyagi M S, 1991, "Introduction to Semiconductor Materials and Devices", New York: Wiley

Xu Y, 1991, "Ferroelectric Materials and their Applications", New York: Elsevier Science Publishing Co. Inc.